


## Autophagy and its mediated mitochondrial quality control maintain pollen tube growth and male fertility in Arabidopsis

He Yan<sup>a</sup>, Menglong Zhuang<sup>a</sup>, Xiaoyu Xu<sup>a</sup>, Shanshan Li<sup>a</sup>, Mingkang Yang<sup>a,b</sup>, Nianle Li<sup>a</sup>, Xiaojuan Du<sup>a</sup>, Kangwei Hu<sup>a</sup>, Xiaomin Peng<sup>a</sup>, Wei Huang<sup>a,b</sup>, Hong Wu<sup>a,b</sup>, Yu Chung Tse<sup>c</sup>, Lifeng Zhao<sup>a</sup>, and Hao Wang <sup>a</sup>

<sup>a</sup>Department of Cell and Developmental Biology, College of Life Sciences, South China Agricultural University, Guangzhou, Hong Kong, China;

<sup>b</sup>State Key Laboratory for Conservation and Utilization of Subtropical Agro-bioresources, South China Agricultural University, Guangzhou null China;

<sup>c</sup>Core Research Facilities, Southern University of Science and Technology, Shenzhen, Guangdong, China

### ABSTRACT

Macroautophagy/autophagy, a major catabolic pathway in eukaryotes, participates in plant sexual reproduction including the processes of male gametogenesis and the self-incompatibility response. Rapid pollen tube growth is another essential reproductive process that is metabolically highly demanding to drive the vigorous cell growth for delivery of male gametes for fertilization in angiosperms. Whether and how autophagy operates to maintain the homeostasis of pollen tubes remains unknown. Here, we provide evidence that autophagy is elevated in growing pollen tubes and critically required during pollen tube growth and male fertility in Arabidopsis. We demonstrate that SH3P2, a critical non-ATG regulator of plant autophagy, colocalizes with representative ATG proteins during autophagosome biogenesis in growing pollen tubes. Downregulation of *SH3P2* expression significantly disrupts Arabidopsis pollen germination and pollen tube growth. Further analysis of organelle dynamics reveals crosstalk between autophagosomes and prevacuolar compartments following the inhibition of phosphatidylinositol 3-kinase. In addition, time-lapse imaging and tracking of ATG8e-labeled autophagosomes and depolarized mitochondria demonstrate that they interact specifically *via* the ATG8-family interacting motif (AIM)-docking site to mediate mitophagy. Ultrastructural identification of mitophagosomes and two additional forms of autophagosomes imply that multiple types of autophagy are likely to function simultaneously within pollen tubes. Altogether, our results suggest that autophagy is functionally crucial for mediating mitochondrial quality control and canonical cytoplasm recycling during pollen tube growth.

**Abbreviations:** AIM: ATG8-family interacting motif; ATG8: autophagy related 8; ATG5: autophagy related 5; ATG7: autophagy related 7; BTH: acibenzolar-S-methyl; DEX: dexamethasone; DNP: 2,4-dinitrophenol; GFP: green fluorescent protein; YFP: yellow fluorescent protein; PtdIns3K: phosphatidylinositol 3-kinase; PtdIns3P: phosphatidylinositol-3-phosphate; PVC: prevacuolar compartment; SH3P2: SH3 domain-containing protein 2.

### ARTICLE HISTORY

Received 11 January 2022

Revised 23 June 2022

Accepted 24 June 2022

### KEYWORDS


Arabidopsis; ATG8e; autophagy; male fertility; mitophagy; pollen tube growth; SH3P2

### Introduction

Unlike most immotile plant cells, pollen tubes exhibit rapid and tip-focused cell expansion to deliver the male gametes to the ovule for fertilization. Rapid growth requires commensurate production and transportation of cellular molecules such as proteins, lipids and cell wall materials toward the tip of the pollen tube where vigorous and polarized cell growth occurs. To empower this robust cell metabolism and drive the fast pollen tube growth, mitochondria are highly enriched in growing pollen tubes [1–6]. Additionally, quick degradation and recycling of damaged cellular components (e.g. mitochondria and proteins) seems to be a more efficient way to meet the requirement of fast pollen tube growth than *de novo* synthesis [5–7]. Vacuole-mediated degradation is one of the major degradation pathways in plant cells [8–10]. Previous studies found that disruption of vacuolar trafficking pathways or vacuole biogenesis strongly inhibits pollen tube germination, growth and fertility [11–13]. However, the underlying machinery underpinning degradation and recycling of proteins, lipids and damaged organelles in rapid growing pollen tubes remains unclear.

Autophagy, an evolutionarily conserved intracellular degradation and recycling pathway in eukaryotes, plays an essential role in regulation of a wide spectrum of physiological processes including cell metabolism, growth, development and senescence [14–17]. Macroautophagy, referred to as autophagy henceforth, is the major type of autophagy that is mediated by the formation of a phagophore that matures into a double-membrane organelle called the autophagosome. Damaged cellular components are first surrounded by the presumptive phagophore membranes, which expand to sequester the cargo. The outer membrane of the mature autophagosome fuses with the tonoplast of the vacuole bringing the inner membrane and contents into the lumen of the vacuole for degradation and turnover [18,19]. The activity of autophagy usually remains at a low housekeeping level, whereas it can be greatly induced when challenged with survival-limiting conditions. Indeed, the majority of our knowledge of autophagy is derived from the context of stress responses, nutrient deprivation and aging. The upregulated autophagic pathway allows for extensive removal and

**CONTACT** Hao Wang  [wanghaohw@gmail.com](mailto:wanghaohw@gmail.com)  College of Life Sciences, South China Agricultural University, Guangzhou 510642, China

 Supplemental data for this article can be accessed online at <https://doi.org/10.1080/15548627.2022.2095838>

© 2022 The Author(s). Published by Informa UK Limited, trading as Taylor & Francis Group.

This is an Open Access article distributed under the terms of the Creative Commons Attribution-NonCommercial-NoDerivatives License (<http://creativecommons.org/licenses/by-nc-nd/4.0/>), which permits non-commercial re-use, distribution, and reproduction in any medium, provided the original work is properly cited, and is not altered, transformed, or built upon in any way.

recycling of cellular materials to cope with harsh conditions in an effort to extend the life of cells [20–22]. In contrast, the regulatory roles of autophagy within the context of cell development and homeostasis such as in pollen tube germination, growth and fertility are less well understood.

Autophagy-related (ATG) proteins have been well characterized as core molecular components which are spatiotemporally orchestrated and regulated to facilitate autophagosomal biogenesis and function in eukaryotes [18,23,24]. Meanwhile, non-ATG proteins are also found to work together with ATGs to regulate autophagy [25–27]. The BAR domain protein SH3P2 (SH3 DOMAIN-CONTAINING PROTEIN 2) has been found to interact with phosphatidylinositol-3-phosphate (PtdIns3P) and ATG8 to regulate autophagosome biogenesis in Arabidopsis. It localizes to the crescent and ring-like autophagic structures upon autophagy induction and is detected on the membrane of autophagosomes [26]. Distinct from animals and yeasts, the majority of the plant *atg* mutants show no obvious deleterious phenotypes during growth and development under regular growth conditions. It is possible that functional redundancy could account for the lack of phenotypes due to the great expansion of *ATG* homology genes in plants [18,28]. Nonetheless, recent studies have indicated that autophagy plays pivotal roles in male gametophyte development and reproduction in several plant species [29–31]. Deletion of *AtATG6* in Arabidopsis and *Osatg7* in rice causes severe defects in male gametophyte development and sterility although their detailed underlying working mechanisms yet to be uncovered [31–35]. Recently, ATG8-mediated autophagy was found to participate in cytoplasmic deletion during pollen germination. Inhibition of autophagy caused the persistence of specific cytoplasm at the germination aperture, which prevents the extrusion of pollen tubes [36]. Whether and how autophagy participates in this intracellular degradation during pollen tube growth and fertility has hitherto remained unresolved.

In this study, we have determined that autophagy critically participates in regulating pollen tube growth for male fertility. Autophagic processes can be significantly elevated in growing pollen tubes. Suppression of autophagy by downregulating the activity of SH3P2 *via* RNAi significantly inhibited pollen tube growth and resulted in male infertility in Arabidopsis. Furthermore, SH3P2-XFP colocalized with various core ATG proteins in the different stages of autophagosome development in pollen tubes. In addition, we have revealed that autophagy functionally mediates depolarized mitochondria removal as well as canonical cytoplasm recycling in growing pollen tubes.

## Results

### **SH3P2 critically participates in pollen germination and pollen tube growth for male fertility**

SH3P2 has been identified to function as an essential molecule that facilitates membrane curvature and interacts with PtdIns3P for biogenesis of autophagosomes in Arabidopsis [26]. In addition, SH3P2 localizes to the leading edge of the cell plate and participates in converting fused vesicles to tubular structures during cytokinesis [37]. The Arabidopsis *sh3p2* knockout mutant is embryo-lethal and downregulation of the

transcription of *SH3P2* by RNAi showed significant arrest of plant development and growth [26]. Furthermore, gene expression profile analysis from the Genevestigator (<https://genevestigator.com/>) showed that *SH3P2* is expressed relatively higher in pollens than the other tissues (Figure S1). Because the function of SH3P2 during pollen tube growth remains an unanswered question, we began this investigation by assessing the physiological roles of SH3P2 in pollen tube growth for male fertility.

We first addressed the general requirement of SH3P2 for pollen tube growth using RNAi methods. Pollen germination and pollen tube growth was assessed *in vitro* using transgenic *sh3p2* RNAi Arabidopsis, which is under the control of the dexamethasone (DEX)-inducible promoter [26]. DEX-treated *sh3p2* RNAi strongly inhibited pollen germination and pollen tube growth compared with that of WT (Figure 1A, B and C). Similar results were observed *in vivo* following DEX application to Arabidopsis pollens on stigmas. *sh3p2* RNAi induction resulted in strong inhibition of pollen tube growth in style and arrest of plant fertilization compared with WT and the mock treated *sh3p2* RNAi line (Figure 1) D and E. Semi-quantitative RT-PCR analysis of *SH3P2* expression levels confirms that the transcription of *SH3P2* was greatly decreased after DEX induction of RNAi compared to WT and controls (Figure 1F). Therefore, we have confirmed that SH3P2 is functionally required for pollen germination and pollen tube growth for male fertility during Arabidopsis reproduction.

### **Autophagy is functionally involved in the regulation of pollen tube growth**

Since SH3P2 is involved in pollen tube growth and has previously been implicated in the development of autophagosomes, we next asked whether autophagy participates in regulating pollen tube growth and, if so, is SH3P2 functionally involved in pollen tube autophagy. We performed real-time fluorescent quantitative RT-PCR (qRT-PCR) to investigate the gene expression profiles of *SH3P2* as well as several core *ATG* genes that function in different developmental stages of autophagosomal formation in Arabidopsis pollen grains and growing pollen tubes (Figure 2A). Our results show that *SH3P2* is increasingly expressed in growing pollen tubes, along with several *ATGs* including *ATG1*, *ATG5*, *ATG6*, *ATG7*, *ATG8e*, *ATG9* and *ATG13a*. In addition, we performed western blot analysis on Arabidopsis germinated pollen tubes and pollen grains using ATG8 antibody (Figure 2B). Notably, the amount of ATG8 conjugation to phosphatidylethanolamine (PE) binding to ATG8 was significantly greater in 4-h germinated pollen tubes compared to pollen grains (Figure 2B). This is important because PE is produced *de novo* during autophagy and demonstrates that the extent of autophagy increases during pollen tube growth. Moreover, we performed qRT-PCR to investigate the expression profiles the same set of genes selected in Figure 2A in 4-h germinated Arabidopsis WT and *sh3p2* RNAi pollen tubes with or without DEX treatment. It showed that *SH3P2* together with the representative core *ATG* genes were greatly downregulated in *sh3p2* RNAi pollen tubes under DEX treatment (Figure 2C). Further western blot analysis on 4-h germinated Arabidopsis WT and *sh3p2* RNAi pollen tubes with or without DEX treatment was performed by using ATG8 antibody. The

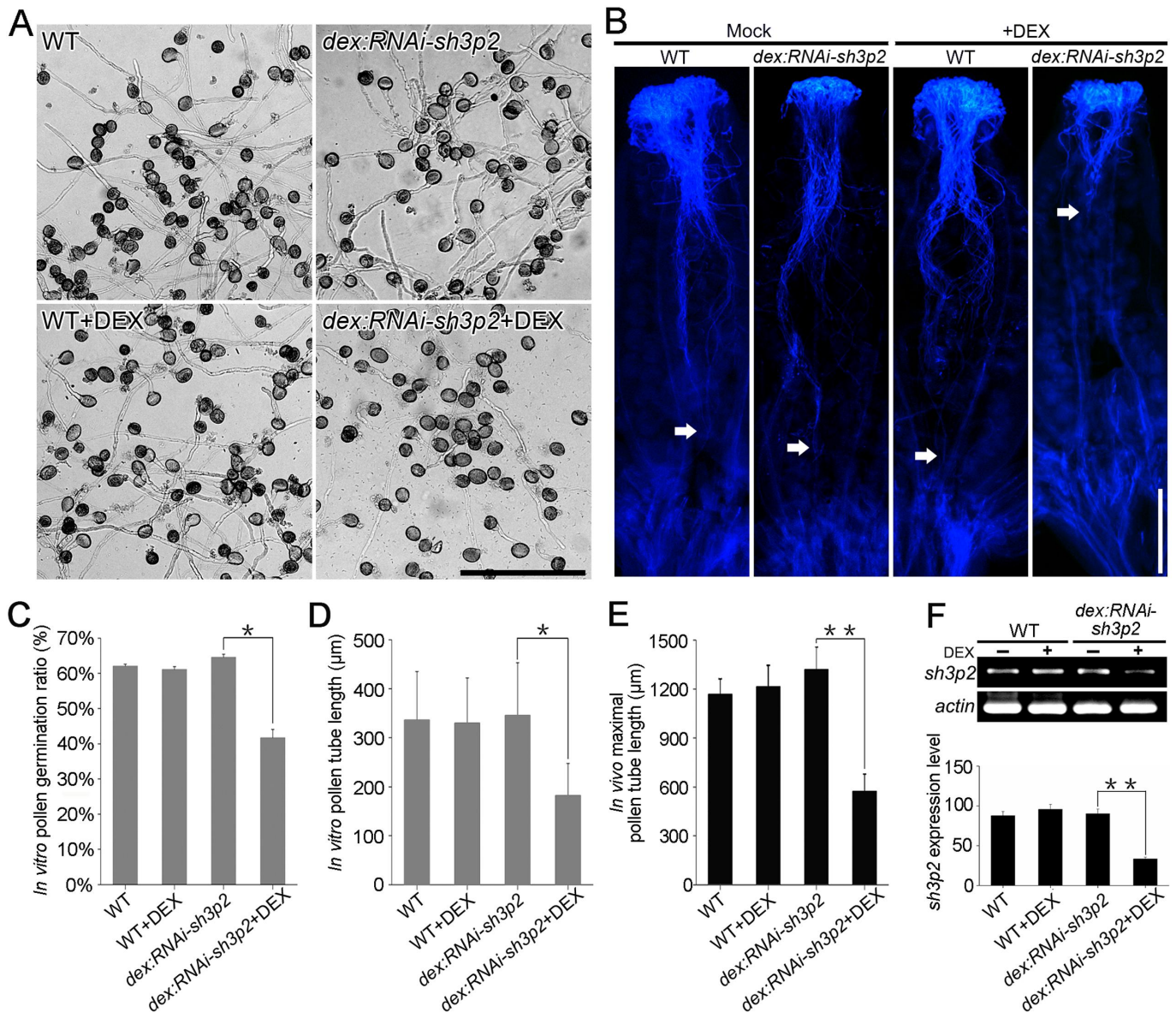


**Figure 1.** SH3P2 is indispensable for pollen tube germination, growth and male fertility. (A) *In vitro* pollen tube germination and growth of Arabidopsis wild type (WT) and SH3P2 RNAi transgenic plant driven by dexamethasone (DEX) inducible promoter. Four-h germinated pollens were performed with or without DEX treatment. Representative images of pollen germination and pollen tube growth are shown. More than 10 independent and 3 times of repeats of samples were observed. (B) Twenty h after pollination, representative images of aniline blue staining of *in vivo* pollen tube germination and growth of WT and *sh3p2* RNAi Arabidopsis with or without DEX treatment. Arrows indicate the positions of the longest pollen tube tip growing in the styles. More than 20 samples were examined in each group. (C) and (D) Statistical analysis of the ratios of *in vitro* pollen germination and measurement of the length of pollen tubes of WT and *sh3p2* RNAi Arabidopsis. \* $p < 0.1$ , *t*-test. (E) Statistical calculation of *in vivo* pollen tube length in the styles. \*\* $p < 0.01$ , *t*-test. (F) Semi-quantitative RT-PCR of SH3P2 expression levels in pollen tubes of WT and *sh3p2* RNAi Arabidopsis with or without DEX treatment. *Actin* transcripts were used as the loading control. \*\* $p < 0.01$ , *t*-test. Data are obtained from 3 independent experiments, with over 30 individual samples analyzed in each statistical experiment. Scale bar in (A): 150 μm and in (B): 300 μm.

amount of ATG8-PE in *sh3p2* RNAi pollen tubes was strongly decreased and barely detectable under DEX treatment (Figure 2D). Taken together, the qPCR and western blot analyses support an upregulated and functional role for autophagy in the regulation of pollen tube growth under regular conditions.

To investigate the subcellular localization and dynamics SH3P2 during pollen tube elongation, we generated a chimeric fluorescent fusion of SH3P2 with YFP and transiently expressed it in growing tobacco pollen tubes (Figure 2E and Movie S1). Punctuate dots of SH3P2-YFP were detected with a cytosolic pattern in growing pollen tubes. To corroborate this observation and correlate the cytosolic localization with autophagy, we made

use of the previously established observation that acibenzolar-S-methyl (BTH) treatment stimulates autophagy in Arabidopsis roots [24]. Different concentrations of BTH were initially tested in order to optimize the pro-autophagy effect and minimize its inhibitory effects on pollen germination and pollen tube growth (Figure S2). We found that 25 μM BTH neither arrests pollen germination nor noticeably disrupts pollen tube growth. The number of SH3P2-YFP dots was greater following BTH treatment for 30 min compared to untreated pollen tubes (Figure 2F, Movie S1). In summary, these results indicate that SH3P2-mediated autophagy occurrence in natural growing pollen tubes and can be stimulated by BTH treatment. Additionally, it



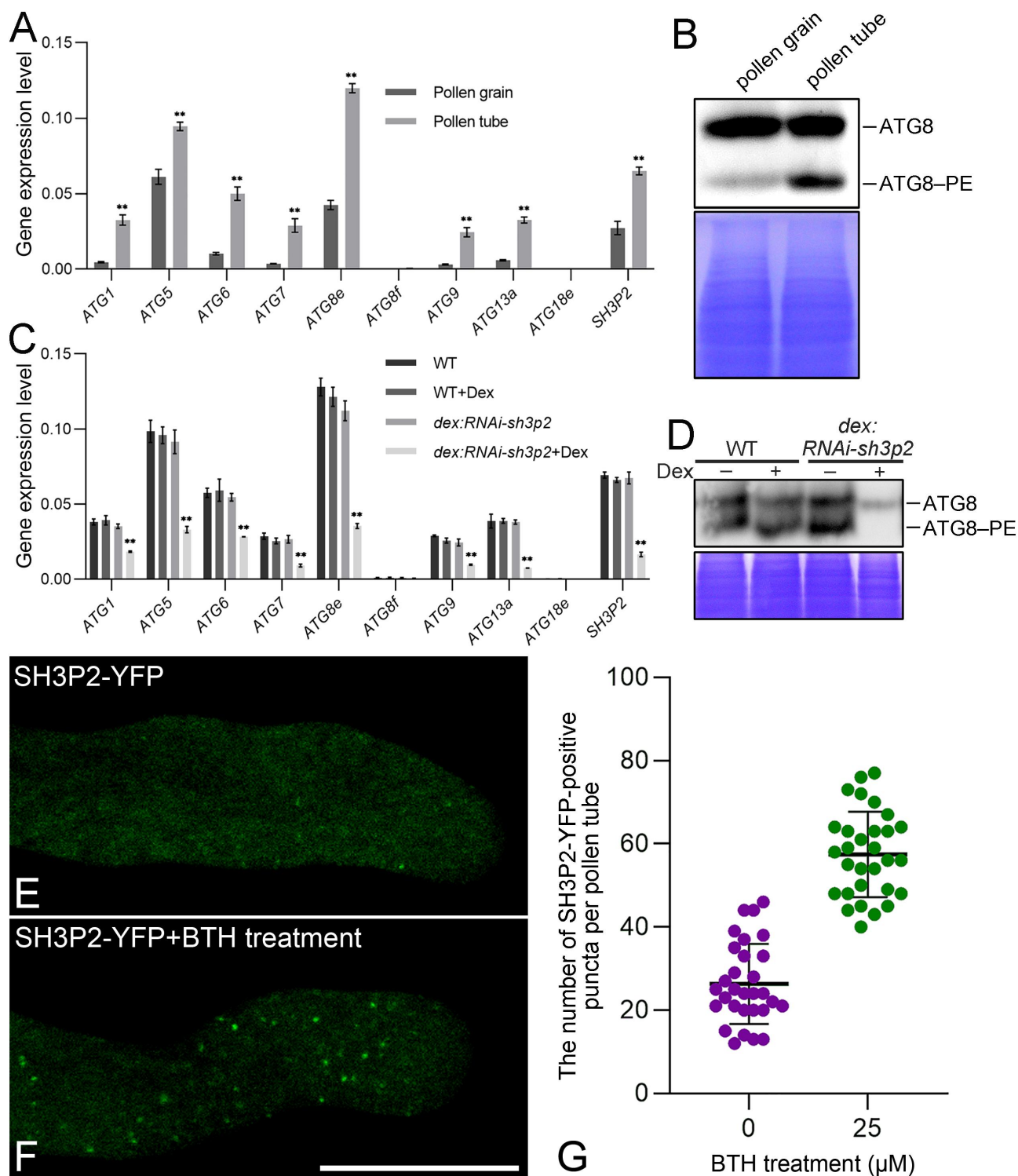


**Figure 2.** Autophagy and SH3P2 participate in pollen tube growth. (A) Transcriptional analysis of *SH3P2* and representative *ATGs* which are involved in different developmental stages of autophagosome biogenesis by qRT-PCR in Arabidopsis pollen grains and 4-h germinated pollen tubes. *Actin* transcripts were used as controls. The results were obtained from four independent repeats (error bars  $\pm$  SD). \*\* $p < 0.01$ , t-test. (B) Western blotting detection of ATG8 and ATG8-PE in Arabidopsis pollen grains and 4-h germinated pollen tubes by ATG8e antibody. (C) Transcriptional analysis of *SH3P2* and representative *ATGs* in 4-h germinated Arabidopsis WT and *sh3p2* RNAi pollen tubes with or without DEX treatment. *Actin* transcripts were used as controls. The results were obtained from four independent repeats (error bars  $\pm$  SD). \*\* $p < 0.01$ , t-test. (D) Western blotting detection of ATG8 and ATG8-PE in 4-h germinated Arabidopsis WT and *sh3p2* RNAi pollen tubes by ATG8e antibody with or without DEX treatment. (E) The subcellular localization of SH3P2 fused with YFP (SH3P2-YFP) driven by the *ubiquitin* (*UBQ*) promoter in tobacco growing pollen tubes. SH3P2-YFP-positive puncta mainly localizes in the shank region of the pollen tube. (F) Expression of SH3P2-YFP in growing tobacco pollen tubes under 25  $\mu$ M BTH treatment for 30 min. The numbers of cytosolic puncta of SH3P2-YFP are significantly greater. (G) Statistical calculation of the numbers of SH3P2-YFP per tobacco pollen tube with and without BTH treatment in 25 independent cells. Scale bar in (E) and (F): 25  $\mu$ m.

is noteworthy that SH3P2 is absent from membrane at the tip of the pollen tube (Figure 2 E and F) when compare with the previous work that characterized an alternative role for SH3P2 in tubulation of secretory vesicles that fuse with the cell plate during cytokinesis [37]. Our results support the conclusion that SH3P2 does not act additionally in apical membrane curvature and maintenance during rapid pollen tube tip expansion.

### **SH3P2 colocalizes with core ATGs and is recruited by ATG8e during autophagosome biogenesis in growing pollen tubes**

To gain a more detailed understanding, we studied the subcellular localization and spatial dynamics of SH3P2-YFP with several representative ATGs that are involved in different

developmental stages of autophagosome formation in growing pollen tubes. SH3P2-YFP-positive puncta mainly colocalized with AtATG1a, AtATG13a, AtATG6, AtATG9, AtATG5 and AtATG7 in growing pollen tubes (Figure 3A-F). Moreover, subcellular localization and dynamic distribution of these proteins were observed in the pollen tube shank (Movies S2A to F).

Besides, some SH3P2 puncta can be actively recruited to ATG8-positive autophagic ring-like structures in growing pollen tubes. ATG8e usually serves as a key autophagic molecule that binds to autophagic lipid membrane and mediates cargo recognition and recruitment to the autophagosomes [18,28]. We found that ATG8e showed two different populations: puncta and ring-like structures in growing pollen tubes (Figure 4A and Movie S3). Furthermore, the number of YFP-ATG8e-positive structures is significantly less compared with

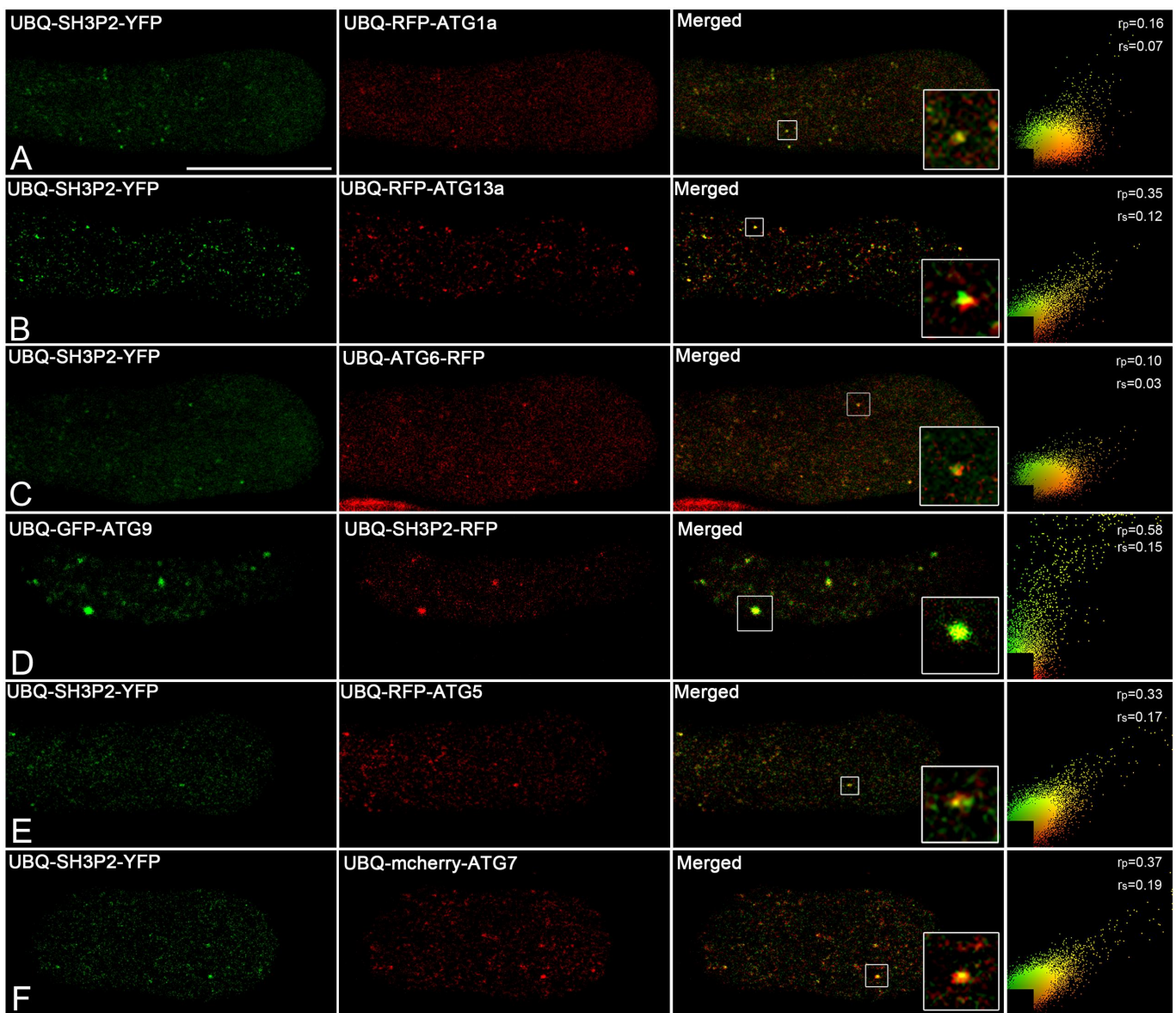


**Figure 3.** SH3P2 colocalizes with representative ATG markers in growing pollen tubes. Coexpression of SH3P2-YFP with several representative ATG markers during autophagosome formation in growing pollen tubes. SH3P2-YFP mainly colocalizes with (A) RFP-ATG1a; (B) RFP-ATG13a; (C) ATG6-RFP; (D) GFP-ATG9; (E) RFP-ATG5; and (F) mcherry-ATG7 in the shank region of growing tobacco pollen tubes. Results of colocalization ratios are calculated by either Pearson correlation coefficients or as Spearman's rank correlation coefficients with image J. The generated  $r$  values in the range  $-1$  to  $1$ , where  $0$  indicates no discernable correlation and  $+1$  or  $-1$  indicate strong positive or negative correlations, respectively. Scale bar in (A)-(F):  $25 \mu\text{m}$ .



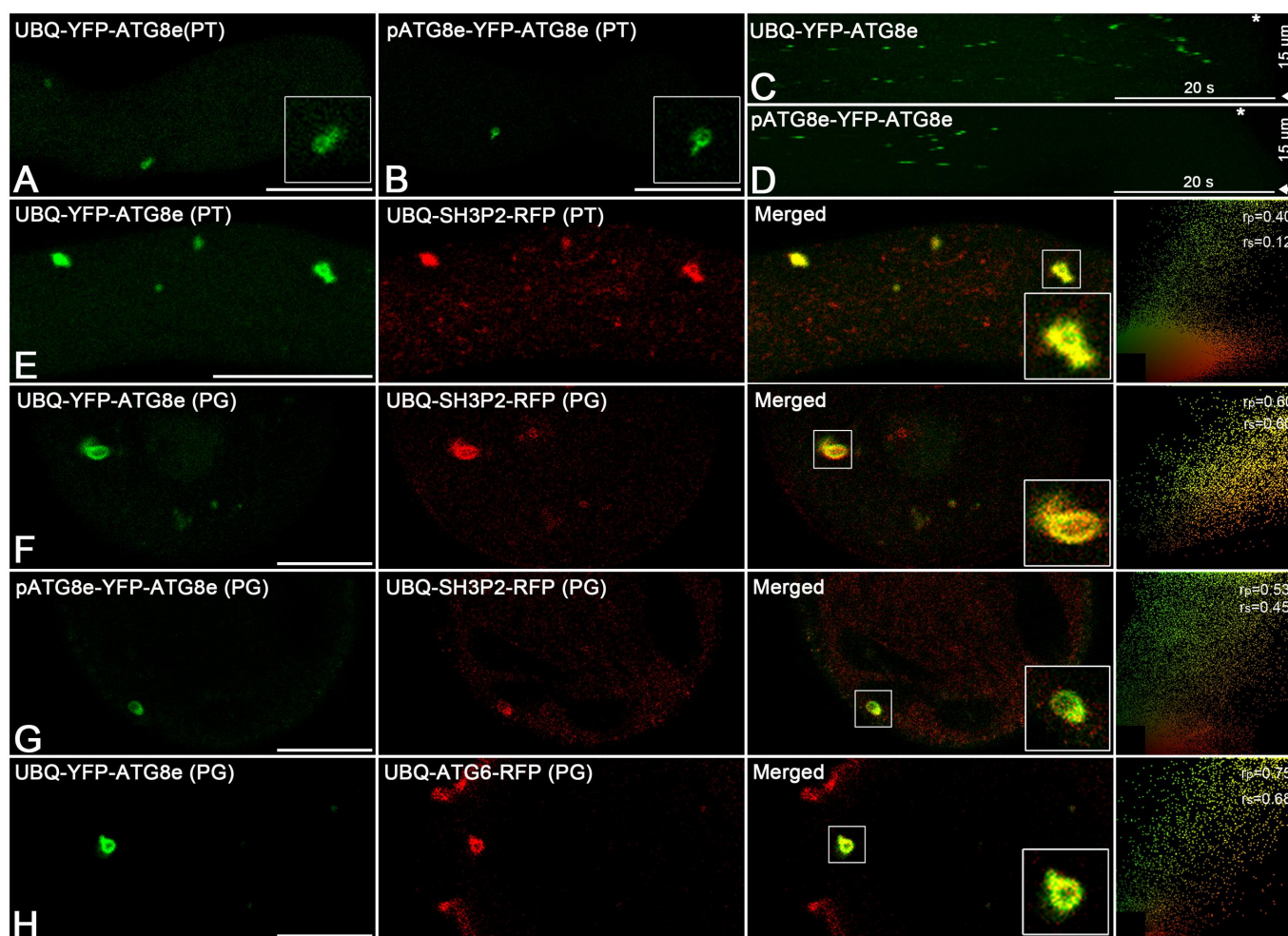


**Figure 4.** SH3P2 is recruited by ATG8 to ring-like autophagosomal structures. (A) and (B) Subcellular localization of YFP-ATG8e driven by *UBQ* promoter and *ATG8e* native promoter (*ATG8ep*) respectively in growing pollen tubes. YFP-ATG8e shows two distinct patterns: cytosolic puncta and ring-like structures. The insets are enlarged images of YFP-ATG8e ring-like autophagosomal structures. (C) and (D) Whole pollen tube kymograph analysis of the spatiotemporal dynamics of YFP-ATG8e shown in (A) and (B). Asterisks and arrows indicate the starting and ending position of the growing pollen tube tip respectively. (E)-(G) Coexpression of YFP-ATG8e with SH3P2-RFP in the growing pollen tube and pollen grain. YFP-ATG8e are driven by both *UBQ* and the *ATG8e* native promoter for expression in pollen tubes and pollen grains. A portion of SH3P2-YFP was recruited to the YFP-ATG8e-positive ring-like autophagosomal structures during coexpression. (H) Coexpression of YFP-ATG8e with ATG6-RFP in germinated pollen grains. ATG6 is recruited to the YFP-ATG8e-positive ring-like autophagosomal structure. Results of colocalization ratios are calculated by either Pearson correlation coefficients or as Spearman's rank correlation coefficients with image J. The generated *r* values in the range -1 to 1, where 0 indicates no discernible correlation and +1 or -1 indicate strong positive or negative correlations, respectively. PT, pollen tube; PG, pollen grain. Scale bar in (A), (B) and (E)-(H): 25  $\mu$ m.

the other ATGs shown in Figure 3. To test for possible ATG8e mislocalization that could be caused by constitutive overexpression driven by the *UBQ10* promoter, we cloned the native promoter of *ATG8e* (*ATG8ep*) to drive the expression of YFP-ATG8e in growing pollen tubes. The results were consistent between these two constructs as shown in Figure 4B and Movie S4. Moreover, kymograph analysis of *UBQ10*- and *ATG8ep*-driven ATG8e expression was performed during pollen tube growth to gain a perspective of its dynamic localization and as a comparison for possible artifacts of overexpression. ATG8e mainly localized in the pollen tube shank but not in the pollen tube tip, an area typically devoid of large organelles such as autophagosome and vacuoles (Figure 4) C and D. Next, we co-expressed YFP-ATG8e with SH3P2-RFP in both growing pollen tubes and pollen grains. YFP-ATG8e fully colocalized with SH3P2-RFP-positive structures (Figure 4) E and F, whereas some SH3P2-RFP remained punctate and separate from ATG8e. Notably, compared to the

SH3P2-RFP puncta observed in pollen tubes (Figure 3), SH3P2-RFP could be recruited and localized to the ring-like autophagosomal structures labeled by YFP-ATG8e when they were coexpressed (Figures 4 E and F). Besides, coexpression of SH3P2-RFP with YFP-ATG8e barely increases the number of ATG8e-positive puncta or ring-like structures (Figure S4). Moreover, the *ATG8e* native promoter was also introduced in the coexpression assay to drive the expression of ATG8e to argue for the possibility that the recruitment of SH3P2-RFP was caused by the overexpression of ATG8e in pollen tubes. A similar result was obtained as shown in Figure 4G.

We further tested coexpression of ATG8e together with ATG6 which has been reported as a critical molecule in regulating pollen germination and male fertility in Arabidopsis [32,34]. Most ATG6 puncta was observed cytosolically while a small fraction was observed to be colocalized with ATG8e-positive autophagosomal ring-like structures (Figure 4H). This result suggests that ATG8e recruits

functional autophagic molecules during the maturation of autophagosomes. Together, SH3P2 colocalizes with various representative autophagic ATG proteins and participates in autophagosome biogenesis in growing pollen tubes.

### **Wortmannin triggers contact between autophagosomes and PVCs**

To further study the spatiotemporal dynamics of SH3P2 and ATG8e during autophagosome formation in growing pollen tubes, we employed wortmannin which is an inhibitor of both the class I phosphoinositide 3-kinase and the class III phosphatidylinositol 3-kinase (PtdIns3K). Disruption of PtdIns3P production has been demonstrated to inhibit biogenesis of autophagosomes [35,38]. In addition, wortmannin can induce homotypic fusion of prevacuolar compartments (PVCs) in plant cells [39–42]. We firstly coexpressed SH3P2-YFP with RFP-2xFYVE, which is a reporter of PtdIns3P and late endosomes in cells [43,44]. In growing pollen tubes, SH3P2-YFP and RFP-2xFYVE were mainly separated with occasional colocalization (Figure 5A). Interestingly, after wortmannin treatment for 30 min, SH3P2-YFP-positive puncta associated with the ring-like structure of enlarged PVCs as shown in Figure 5B. Fluorescent signal intensity analysis (Figure 5B inset image) demonstrated that SH3P2-YFP contacted and resided on the membrane of enlarged PVCs (Figure 5C). The dynamic association and interaction between SH3P2-YFP and an enlarged PVC is shown as a time-lapse series in Figure 5D.

Similarly, YFP-ATG8e associated with the membrane of the enlarged PVCs after wortmannin treatment, whereas they mainly remained separated in growing pollen tubes without treatment (Figure 5) E and F. Two representative areas of Figure 5F were selected and enlarged as Figure 5Fi and Fii. Time-series imaging of the dynamic connection between ATG8e and the membrane of enlarged PVC rings is shown in Figure 5G. Furthermore, the dynamic paths of the ATG8e and the PVCs after wortmannin treatment were computationally tracked, analyzed and modeled by the Imaris software. Their spatiotemporal dynamics were highly accordant as shown in Figure 5H. The results of fluorescent signal intensity and colocalization analysis of the enlarged image shown in Figure 5Fi are shown in Figure 5 I and J respectively.

### **ATG8 interacts with depolarized mitochondria in growing pollen tubes**

Our data reveals the biogenesis of autophagosomes during pollen tube growth. However, what is the biological role of autophagy during this process? We know that large numbers of mitochondria are required for rapidly growing pollen tubes to support the energy demands of metabolism, cell growth and transport related functions [2,5–7]. The autophagy of mitochondria as a general means of cellular quality control is also a well-studied phenomenon. Therefore, we began our analysis by imaging mitochondria within a growing pollen tube stained with MitoTracker for 30 min (Figure 6A). To determine whether mitochondria associate with autophagosomes, we transiently expressed YFP-ATG8e in growing pollen tubes stained with MitoTracker (Figure 6B). The subcellular localizations of ATG8e-positive puncta were mostly

separate from the mitochondria although occasional colocalization occurred as shown by the enlarged images in Figure 6B.

We further treated growing pollen tubes with 2,4-dinitrophenol (DNP), which is often used to induce mitochondrial membrane depolarization and autophagy of the dysfunctional mitochondria (mitophagy) in animals [45]. Moreover, DNP induces mitophagy in Arabidopsis roots [46]. Dosage tests revealed that 6.25  $\mu$ M DNP resulted in the desired effect and minimum toxicity and inhibitory effects on pollen tube growth (Figure S3). Growing pollen tubes expressing YFP-ATG8e and stained with MitoTracker were then subjected to 6.25  $\mu$ M DNP treatment for 30 min. The conditions led to the observation of YFP-ATG8e labeled puncta associated with the depolarized mitochondria which become shortened (Figure 6) C and D compared to those shown in Figure 6A. Time-lapse imaging of YFP-ATG8e and the depolarized mitochondrion in the growing pollen tube is shown their spatiotemporal dynamics (Figure 6E and Movie S5). Tracking and computer modeling followed by kymograph analysis reveals they are not only closely associated but they move in a dynamic, coordinated path (Figure 6 F and G).

In addition, selective autophagy can be achieved through ATG8 recognition and interaction with a cargo-associated ATG8 family-interacting motif (AIM) [18,47]. The AIM-docking site and the potential key amino acids for ATG8 were previously identified in potato (ATG8CL) [47]. Therefore, we compared the ATG8 sequences from several representative species including yeast, human, *C. elegans* and Arabidopsis with that of potato ATG8. Four highly conserved amino acids (ERKR) were selected as amino acids that likely function critically in the AIM-docking site (Figure 6H). We then substituted these amino acids in Arabidopsis ATG8e (E19A R30A K48A R69A) and generated a chimeric fluorescent fusion protein expression vector as shown in Figure 6I. We found that the subcellular localizations and dynamics of GFP-ATG8e (E19A R30A K48A R69A) and the depolarized mitochondria were distinct and remained separate in growing pollen tubes under DNP treatment (Figure 6J, Movie S6). Additional kymograph analysis failed to show association or coordination between the mutant ATG8e construct and depolarized mitochondria (Figure 6K). These observations suggest that depolarized mitochondria specifically associated with autophagosomes *via* binding between ATG8e and AIM. The likely outcome of this association is mitophagic degradation.

### **Ultrastructural identification of three types of autophagosomes in growing pollen tubes**

To visualize the content of growing pollen tubes, including the identification of autophagosomes, at high resolution, we employed electron microscopy. The regular growing Arabidopsis pollen tube specimens were prepared by high pressure freezing and freeze substitution. Ultrathin section and structural identification of autophagosomes in growing pollen tubes were performed. A representative overview image of a pollen tube which contains a large number of mitochondria is shown in Figure 7A. An enlarged image of the structures of mitochondria in the pollen tube is shown in Figure 7B. A representative mitophagosome clearly showing a mitochondrion inside the lumen of a double-membrane autophagosomal structure is shown in Figure 7C. The number of mitophagosomes in pollen tubes decreased



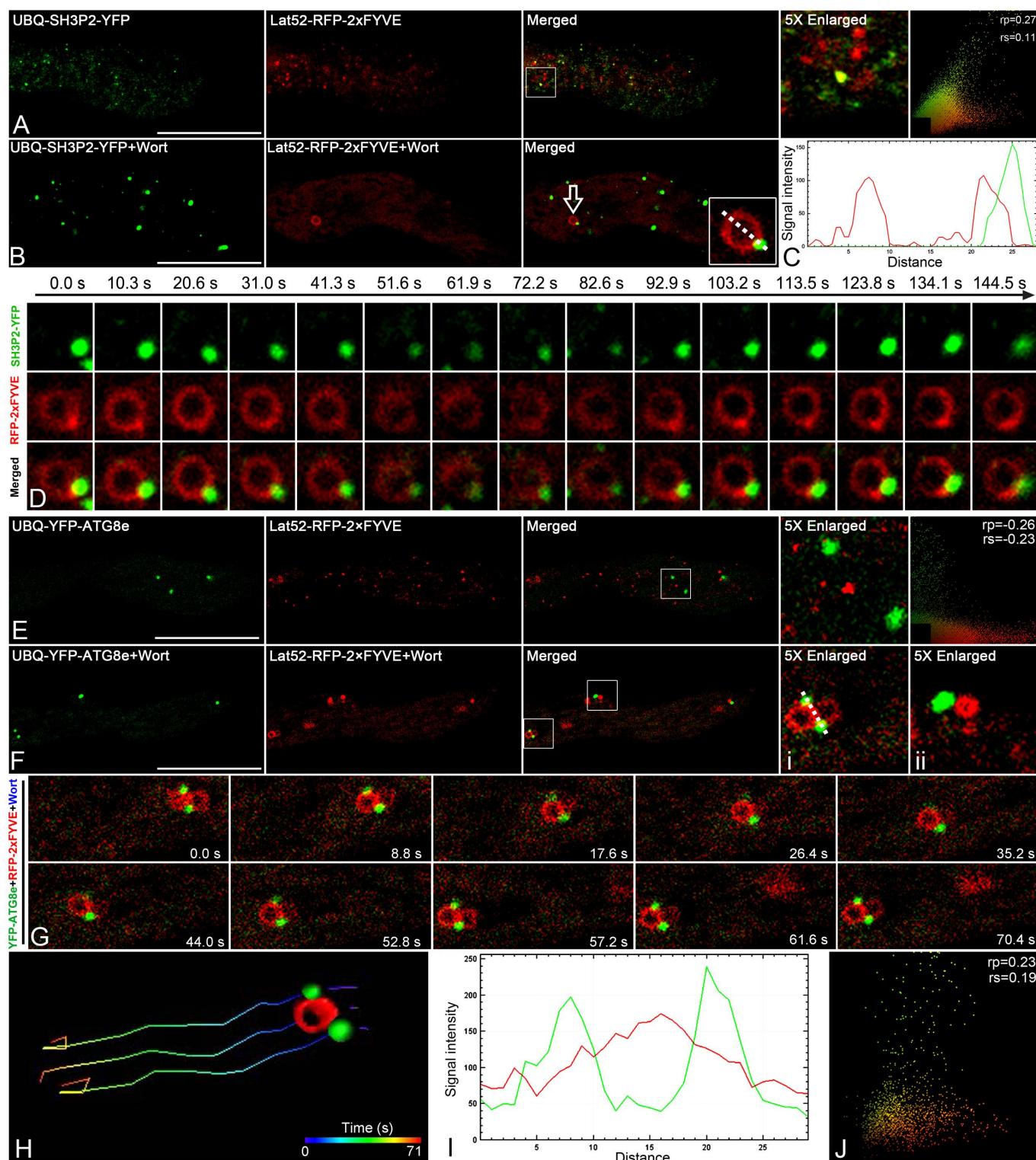


**Figure 5.** Wortmannin induces dynamic interactions of SH3P2 and ATG8e with PVCs in pollen tubes. (A) Coexpression of SH3P2-YFP with RFP-2XFYVE in growing pollen tube. SH3P2-YFP-positive puncta separated from RFP-2XFYVE labeled prevacuolar compartments (PVCs). (B) After 8.25  $\mu$ M wortmannin treatment for 30 min, SH3P2-YFP still remain as puncta, whereas RFP-2XFYVE labeled PVCs form enlarged ring-like structures by homotypic fusion. SH3P2 associate with the enlarged PVC. (C) Fluorescence-intensity analysis of the interaction of SH3P2-YFP with enlarged PVC as shown in the inset image of (B). (D) Representative time-lapse imaging of the dynamic interaction of SH3P2-YFP with enlarged PVC after the wortmannin treatment. (E) Coexpression of YFP-ATG8e with RFP-2XFYVE in growing pollen tube. They mainly remain separated. (F) YFP-ATG8e-positive puncta interact and associate with enlarged PVCs in the growing pollen tube after wortmannin treatment. (G) Representative time-lapse imaging of the spatiotemporal association of YFP-ATG8e with enlarged PVCs in the growing pollen tube after wortmannin treatment. (H) Computational tracking and remodeling of the dynamics of SH3P2 interacting with enlarged PVC under wortmannin treatment in pollen tubes. (I) and (J) Fluorescence-intensity analysis and colocalization calculation of SH3P2 and enlarged PVC shown in (Fi). *Lat52*: a pollen-specific promoter. Scale bar: 25  $\mu$ m.



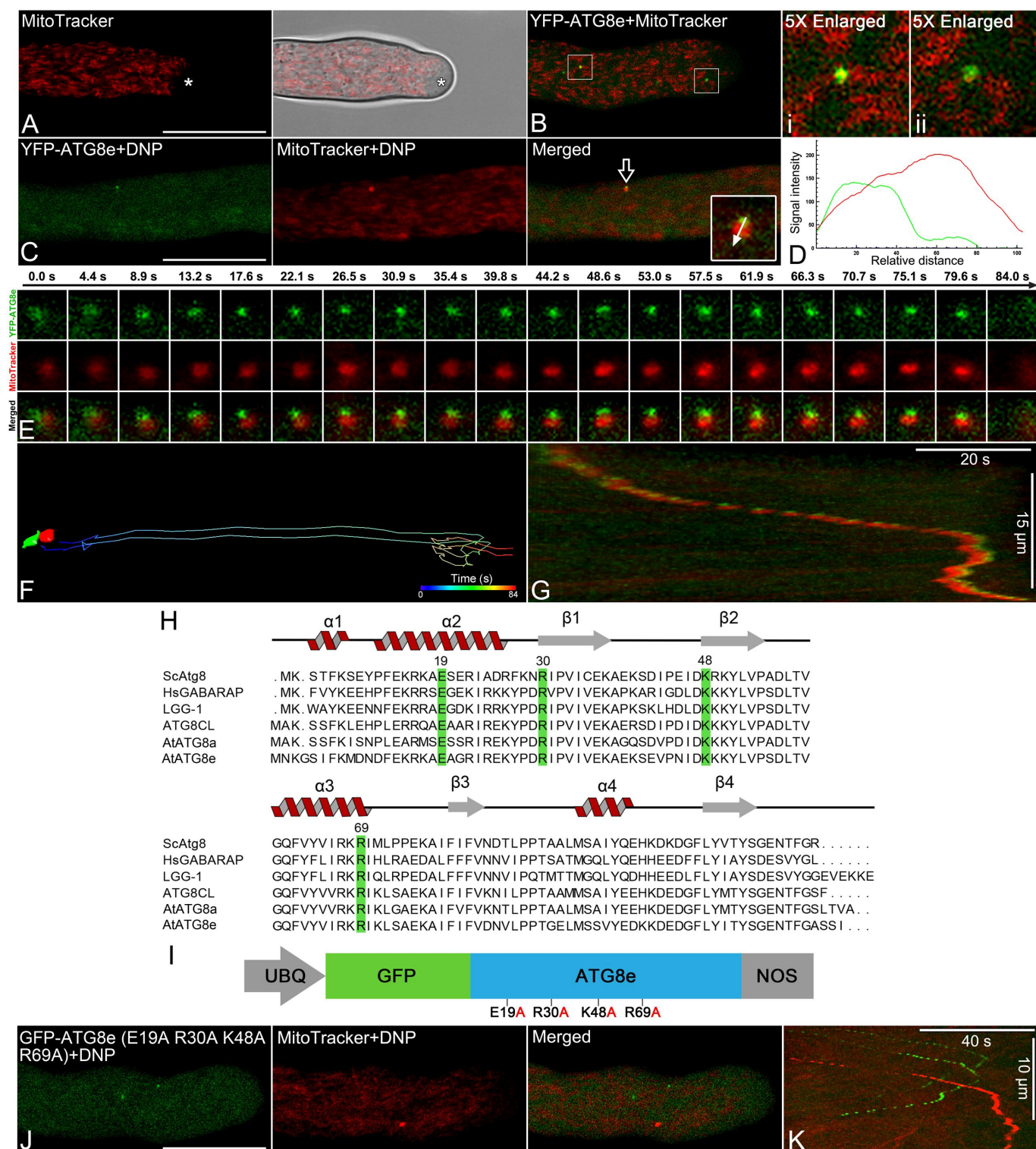


**Figure 6.** Spatiotemporal interaction of autophagosomes with damaged mitochondria in growing pollen tubes. (A) A representative image of a growing pollen tube stained with MitoTracker for 30 min. The asterisk indicates the tip region where mitochondria are typically absent. (B) A growing pollen tube stained with MitoTracker and expressing YFP-ATG8e. The subcellular localizations of most ATG8e-positive puncta were distinct from mitochondria, shown in enlarged image Bi. Occasional colocalizations of ATG8e-positive puncta with mitochondria were also observed as shown in enlarged image Bii. (C) A representative image of a pollen tube stained with MitoTracker and expressing YFP-ATG8e was treated with DNP for 30 min. Dynamic interaction between YFP-ATG8e and the depolarized mitochondrion is indicated by the arrow and enlarged in the inset. (D) Measurement of the fluorescent signal intensity and distribution of the YFP-ATG8e and the damaged mitochondrion shown in the inset. (E) Time-lapse images of the dynamic interaction of ATG8e with the damaged mitochondrion during pollen tube growth. (F) Computational tracking and modeling of the spatiotemporal dynamics of YFP-ATG8e (green) and the depolarized mitochondrion (red) in the growing pollen tube. (G) Kymograph analysis of dynamic association between the YFP-ATG8e and the depolarized mitochondrion in growing pollen tubes. (H) Sequence alignment of ATG8 from several representative eukaryotes including potato ATG8 (ATG8CL). The amino acids of the potential AIM-docking site highlighted in green are highly conserved with those previously identified in ATG8CL. (I) Generation of a chimeric fluorescent fusion of mutated Arabidopsis ATG8e within which the potential key amino acids of the AIM-docking site were substituted (E19A R30A K48A R69A). (J) The subcellular localizations of GFP-ATG8e (E19A R30A K48A R69A) and mitochondria under DNP treatment for 30 min in growing pollen tubes. (K) Kymograph analysis of spatiotemporal kinetics of GFP-ATG8e (E19A R30A K48A R69A) and the damaged mitochondrion in growing pollen tubes. Scale bar in (A), (C) and (J): 25  $\mu$ m.



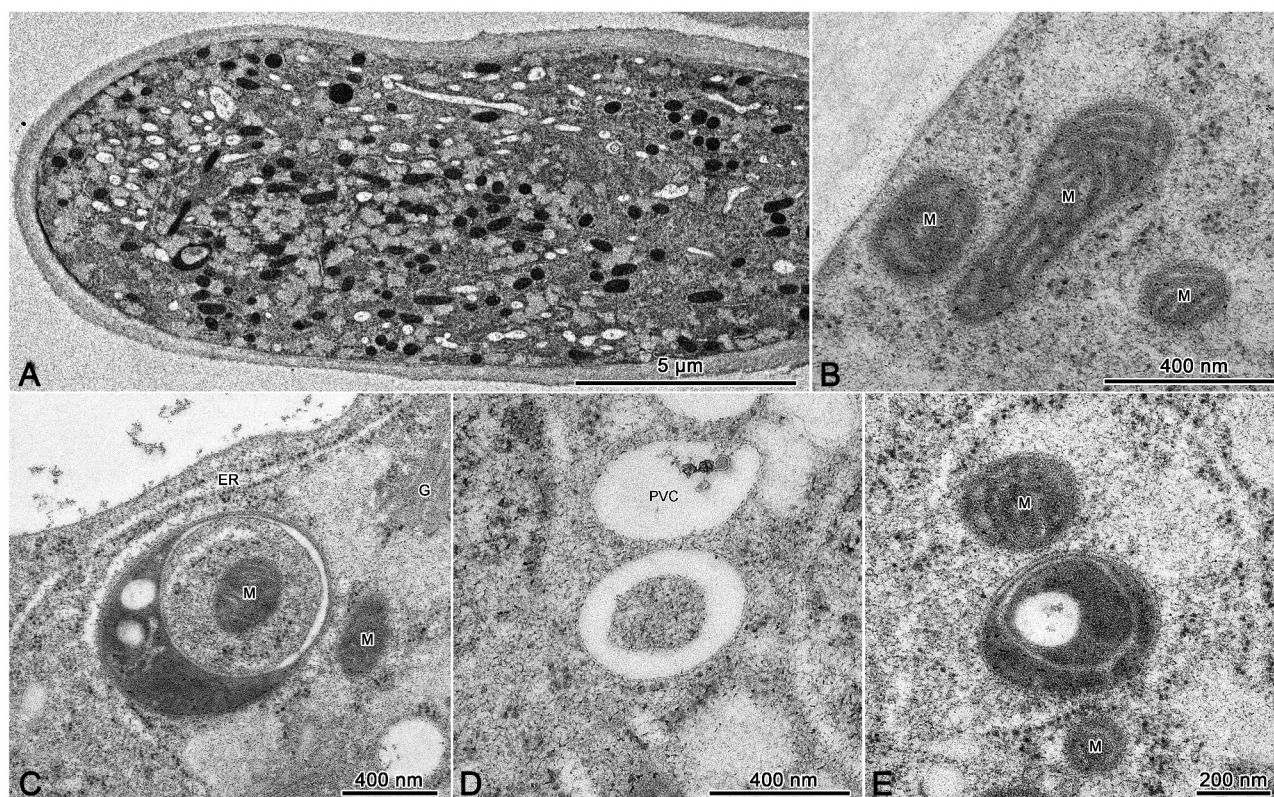


**Figure 7.** Ultrastructural identification of mitophagosomes and other types of autophagosomes in pollen tubes. 4-h germinated *Arabidopsis* pollen tubes were fixed and prepared by high pressure freezing and freeze substitution. (A) A representative overview image of the ultrathin structure of a pollen tube. (B) Typical structures of mitochondria in pollen tubes. (C) A representative image of a mitophagosome in the pollen tube. A mitochondrion was enclosed within a double-membrane autophagosomal structure. Meanwhile, double-membraned autophagosomes with either cytosol (D) or fragmented membrane elements inside (E) were also observed in pollen tubes. M, mitochondrion; PVC, prevacuolar compartment; G, Golgi apparatus; ER, endoplasmic reticulum.

significantly in *sh3p2* RNAi pollen tubes after DEX induction (Figure S4). In addition, autophagosomes containing cytoplasmic content (Figure 7D) and fragmented membranes in the lumen (Figure 7E) were also found in *Arabidopsis* growing pollen tubes. Therefore, three types of autophagosomes are represented in growing *Arabidopsis* pollen tubes.

Our results concerning the role of autophagy in the regulation of *Arabidopsis* pollen tube growth are summarized in a simplified schematic diagram (Figure 8). We conclude that rapid degradation and recycling of the intracellular materials including organelles, proteins, lipids and sugars by autophagy play essential roles in supporting the fast pollen tube growth. Three types of autophagosomes were found and coexist in growing *Arabidopsis* pollen tubes including mitophagosomes. Therefore, different types of autophagosomes with distinct metabolic purposes coexist and function together to regulate pollen tube growth for male fertility in *Arabidopsis*.

## Discussion

### *SH3P2* participates in autophagy and regulates pollen tube growth in *Arabidopsis*

SH3P2 is not an ATG protein but plays a role in the biogenesis of plant autophagosome *via* coordination with PtdIns3P and ATG8 to facilitate the formation and closure of autophagosomes in *Arabidopsis*. Downregulation of SH3P2 strongly

inhibits plant development and growth, impairs autophagy pathway and causes accumulation of unwanted cellular components in vacuoles. Therefore, SH3P2 functions as a pivotal regulatory protein during autophagosome biogenesis in *Arabidopsis* [26]. In addition to its role in autophagy, SH3P2 functions in cell plate formation during cytokinesis in *Arabidopsis* root cells. It localizes to the leading edges of the developing cell plate to form a complex with DRP1 which functions in tubulation of vesicles and maintenance of the cell plate shape during cell division [37]. Therefore, SH3P2 plays distinct roles in non-dividing and dividing cells in *Arabidopsis*.

In our study, downregulation of *SH3P2* expression significantly inhibited pollen tube germination, growth and male fertility in the transgenic *Arabidopsis* line expressing *SH3P2* RNAi under the control of the DEX-inducible promoter (Figure 1). This result indicates that SH3P2 serves as a crucial molecule in regulating pollen tube growth during *Arabidopsis* sexual reproduction (Figure 1). Two processes of pollen tube formation fit the functional characteristics of SH3P2: recycling of cellular materials by autophagy, maintenance of the growing root tip apical dome or both. To decide between these three possibilities, we generated a SH3P2-YFP chimera and characterized its subcellular localizations in growing pollen tubes. SH3P2-YFP-positive puncta mainly localized in the shank and, importantly, was absent from the tip of the pollen tubes (Figure 2). Moreover, SH3P2-YFP colocalized with various core ATG proteins that are involved



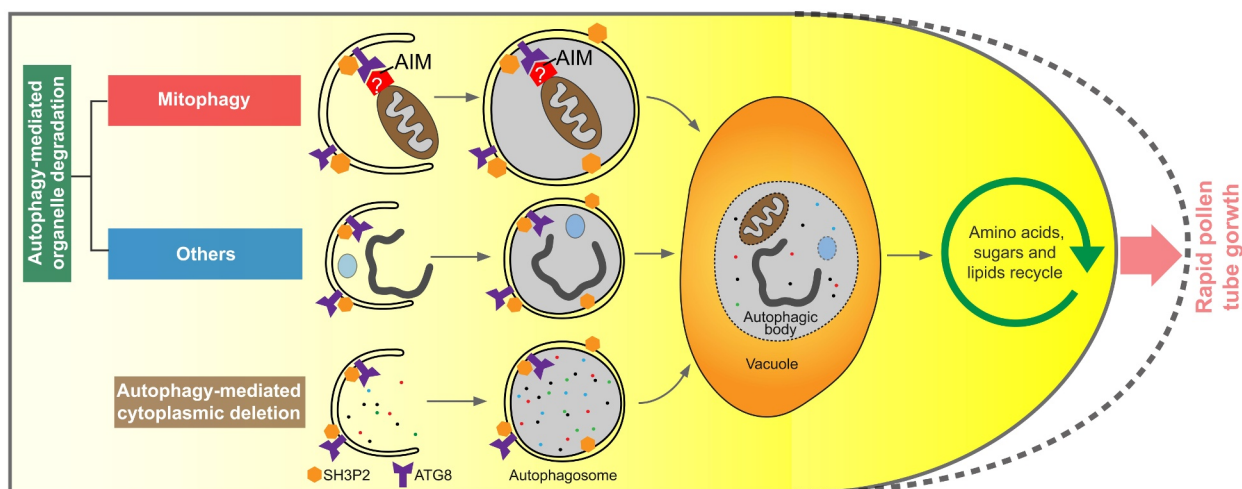


**Figure 8.** Schematic representation of autophagy pathways during pollen tube growth. Rapid degradation and recycling of cellular materials are critical to maintain the fast growth of pollen tubes and functions. Autophagy as one of the major pathways for degradation and turnover of cellular components participates in regulating pollen tube growth for male fertility in Arabidopsis. A simplified schematic diagram is proposed to demonstrate the possible roles of autophagy during pollen tube growth. The depolarized mitochondria are specifically reorganized and bound with ATG8 via AIM-docking site for mitophagy, although the AIM-containing mitochondrial protein(S) remain to be further determined. Moreover, autophagy could also participate in fragmented membrane removal and cytoplasmic deletion in growing pollen tubes. Among various autophagic regulators and effectors, SH3P2 and ATG8 are likely to serve as key molecules and participate in different types of autophagy in regulating biogenesis and functions of autophagosomes during pollen tube growth.

in different stages of autophagosome biogenesis. From these results we conclude that: (i) SH3P2 localizes on autophagic compartments and participates in autophagy within growing pollen tubes (Figure 3 and 4); (ii) SH3P2 does not directly participate in pollen tube tip morphogenesis and polarization; and (iii) SH3P2 serves as a useful reporter of autophagy in growing pollen tubes.

### Autophagy is functionally active during pollen tube growth in Arabidopsis

Emerging evidence from a few plant species suggests that autophagy participates in regulating multiple developmental processes of plant sexual reproduction, including the self-compatibility response, anther development, male gamete fertility and pollen germination [15,29,30,32,33,36,48–53]. Mutation of *AtATG6* in Arabidopsis and *OsATG7* in rice both showed sterility due to strong defects in male gamete fertility [29,32–34]. However, it remains in debate that whether autophagy actually plays a functional role in Arabidopsis male reproduction since *AtATG6* meanwhile serves as an essential component of the PtdIns3K complex. In spite of autophagy, multiple cellular activities including endocytosis, endomembrane trafficking and intracellular signaling critically require involvement of PtdIns3K. Moreover, most of Arabidopsis *atg* mutants showed no obvious defects in sexual reproduction and that expression levels of *AtATGs* were found to be significantly lower in mature pollen compared to the other vegetative tissues [48]. In particular, pollen germination and plant reproduction in Arabidopsis *atg5* and *atg7* mutants do not show phenotypes distinct from wild type under regular cultivation conditions whereas the pollen germination ratio was greatly reduced in *atg5* and *atg7* RNAi tobacco plants [36]. These different phenotypes between Arabidopsis and tobacco are possible due to the spatiotemporal occurrence and functional roles of autophagy during plant reproduction and could vary

across different plant species. Moreover, it is important to note that impaired pollen development and male sterility were significantly increased in Arabidopsis *atg2*, *atg5*, *atg7* and *atg10* mutants under high-temperature stress [15]. Thus, it suggests that *ATG5* and *ATG7* actually regulate male gametophyte development under heat stress in Arabidopsis.

While these observations have cast doubt on a substantial role for canonical autophagy in male gametophyte development and fertility in Arabidopsis, our results elucidate its critical importance in pollen tube growth. Herein we describe several lines of evidence. First, the expression profile of *SH3P2* and several representative *ATGs* were examined in 4-h germinated pollen tubes. We found that *SH3P2* as well as several core *ATGs* including *ATG5* and *ATG8e* are highly expressed in pollen tubes (Figure 2 and Figure S2). Second, the contents of both ATG8 and ATG8-PE were significantly increased in pollen tubes compared to mature pollen detected by ATG8 antibody (Figure 2), suggesting that the autophagic level was substantially stimulated in growing pollen tubes compared to pollen grains. Third, downregulation of *SH3P2*, which functions as a key molecule mediating autophagosome biogenesis dramatically inhibited pollen germination, pollen tube growth and male fertility (Figure 1). Fourth, ATG8e-positive autophagic compartments specifically interacted with depolymerized mitochondria relying on the ATG8-interacting motif (AIM)-docking site (Figure 6). Finally, mitophagosomes were morphologically identified in pollen tubes by TEM (Figure 7). Together, these results suggest that autophagy is functionally represented during pollen tube growth and male gamete fertility in Arabidopsis.

In fact, the regulatory roles of autophagy have been revealed in tobacco pollen. Zhou *et al.* demonstrated that the expression level of most *NtATG* genes was greater in mature pollen compared with other tissues [48,54]. Furthermore, they showed that autophagy mediates compartmental cytoplasmic removal to initiate tobacco

pollen germination. Inhibition of autophagy caused a persistence of undegraded cytoplasm at the germination aperture inhibiting pollen germination [36]. Consistent with this report, we found a population of autophagosomes containing cytoplasm in Arabidopsis pollen tubes by TEM ultra-structural imaging (Figure 7). This identification suggests that autophagy-mediated cytoplasmic deletion occurs during Arabidopsis pollen tube growth. Whether autophagy plays a role during Arabidopsis pollen germination similar to that observed in tobacco needs further investigation.

### **Subcellular localizations and spatiotemporal dynamics of autophagosomes in growing pollen tubes**

Our live cell imaging of growing pollen tubes expressing fluorescent protein-tagged core ATG proteins including AtATG6, AtATG8e and AtATG9 showed that they all localized in the shank region while absent from the tip, which is mainly populated by exo/endocytic vesicles (Figure 3 and 4). Interestingly, Zhao *et al.* demonstrated that ATG8 was localized in the emerging tip of the pollen tube at the germination aperture *via* immunofluorescent labeling with ATG8 antibody [36]. The ATG8-mediated autophagy is mainly responsible for formation of autophagosomes containing cytoplasm and subsequent degradation at the site of pollen germination to allow pollen tube extrusion. The distinct subcellular localizations of ATG8 during pollen tube germination and pollen tube growth may be due to diverse functions of autophagy at different cell developmental stages in plants. In addition, we identified autophagosomes containing cytoplasm within Arabidopsis pollen tubes by TEM ultra-structural imaging, though their specific functions within this context remain to be characterized (Figure 7). Mitophagosomes and autophagosomes containing membrane fragments were also observed in growing Arabidopsis pollen tubes (Figure 7) suggesting that multiple types of autophagy coexist and function together in regulating pollen tube growth.

With regards to the observation of mitophagosome ultrastructures, we provide evidence that the interaction between ATG8e and depolarized mitochondria is specifically mediated by the AIM-docking site of ATG8e in growing pollen tubes (Figure 6). Mutation of highly conserved amino acids that likely function as the AIM-docking site disrupted the dynamic coincidence between ATG8e and the depolarized mitochondria (Figure 6) While the ATG8e-binding AIM protein(s) on mitochondria remain yet to be characterized and studied, our results through a functional analysis provide an important data point for its presence and activity. Furthermore, a recent study found that ATG8 interacts through an alternative binding site with a new set of candidates that contain a ubiquitin-interacting motif (UIM) other than the canonical AIM. Identification of the ATG8-binding UIM proteins reveals a new type of selective autophagy pathway in plants, yeasts and humans [36]. It further suggests that ATG8 could interact with diverse types of cargo proteins to regulate different classes of autophagic pathways in eukaryotic cells. Thus, distinct internal contents of autophagosomes including mitophagosome found in our study (Figure 7) indicates that a diversity of autophagy-mediated cargo selection and recycling exist in growing pollen tubes. Further detailed study of tissue/cell specific ATG8 family

protein(s) will advance our understandings of the diverse functions of ATG8s in autophagy in plants.

### **Inhibition of PtdIns3P induced the interaction between autophagosomes and PVCs**

Autophagosomes and late endosomes/PVCs are two morphologically distinct organelles that mediate lysosomal and vacuolar degradation pathways, respectively, in eukaryotes [18,40,41]. Additionally, fusion of these two organelle types has been observed, resulting in an amphisome in yeast and animal cells [36,55]. Similar fusion events have also been observed and reported in plant cells in recent years [55,56]. The mechanistic details of these hybrid organelles remain unclear. In our study, wortmannin treatment of pollen tubes coexpressing SH3P2-YFP or YFP-ATG8e with RFP-2xFYVE induced interaction and dynamic association of autophagosomes/phagophores with enlarged PVCs (Figure 5). Wortmannin, an extensively used PtdIns3K inhibitor, can inhibit autophagy by preventing the production and recruitment of PtdIns3P to the phagophore membrane [53,57,58]. Although the mechanism is not well understood, wortmannin can also induce homotypic fusion of PVCs in plants [39,40,42,59]. PtdIns3P is a critical molecule for recruiting various autophagic proteins including ATG8 and SH3P2 to the phagophore membrane to facilitate the formation of autophagosomes [60]. In addition, PtdIns3P is highly enriched in the membrane of late endosomes/PVCs in plant cells. Chimeric fluorescent fusion of 2xFYVE, which serves as a specific biosensor for visualization of PtdIns3P, is mainly detected on PVCs [61]. PtdIns3P serves as a shared and key molecule that is involved in both autophagy and the PVC pathway for vacuolar degradation. Inhibition of PtdIns3P production by wortmannin could induce the interplay between the autophagosomes and the enlarged PVCs in growing pollen tubes, implying PtdIns3P might serve as a possible link during the conversion of autophagosome and PVC.

Another protein shown to affect the biogenesis and function of autophagosomes and PVCs is FYVE domain protein required for endosomal sorting 1 (FREE1), which is an ESCRT complex-associated protein that is unique to plants [56,62]. The Arabidopsis *free1* mutant showed significant increased accumulation of autophagosomes and association between autophagosomes and PVCs [56]. In addition, immunoprecipitation assays showed that FREE1 could interact with PtdIns3K components and SH3P2, which collaborates with ATG8 in regulating autophagosome formation [26,56]. This finding suggests that FREE1 is likely to function along with the PtdIns3K complex, SH3P2 and ATG8 during autophagy. Therefore, production of PtdIns3P at the site of autophagosome formation is a required process for the recruitment of various autophagy regulators. Meanwhile, the diverse roles of PtdIns3P involved in multiple endosomal processes may position PtdIns3P as a central link for the interplay between autophagosomes and other organelles [60]. For example, Kim *et al.*, recently demonstrated that cell death-related endosomal FYVE/SYLF protein 1 (CFS1/FYVE2), a PtdIns3P effector that participates in COPII vesicle formation from ER through an interaction with SAR1 GTPase also interacts with autophagic protein ATG18a on the phagophore



membrane [63]. Mutation of CFS1/FYVE2 or SAR1B caused the accumulation of autophagic organelles in plant cells [63]. Looking forward, further detailed studies will be needed to investigate the coordination of PtdIns3P, SH3P2, ATG8 and FREE1 for crosstalk between autophagosomes and PVCs in plants.

### Occurrence of mitophagy in growing pollen tubes

Selective autophagy of mitochondria, also known as mitophagy, is one of the major quality control pathways to maintain a functional mitochondrial network in cells [64,65]. The mitophagy pathway has been well established through the identification of critical molecules and the mechanisms have been extensively studied in yeast and animals. However, research into plant mitophagy is still in its infancy, in part due to the fact that many of the key factors involved in mitophagy in yeast and animals are absent from plants.

Pollen tubes are one of the fastest growing cell types in nature. To support the rapid and sustainable pollen tube growth, high levels of energy production is required to support the active metabolism and vigorous intracellular transport [2,4,5]. The number of mitochondria in pollen is about 20-fold greater compared to vegetative cells in maize [66]. A great number of mitochondria was also observed in *Arabidopsis* pollen tubes (Figure 7), consistent with reports of their high metabolic demands [1,2,7]. It remains largely unknown how the quality and quantity of healthy mitochondria are maintained and whether mitophagy serves as a crucial pathway to mediate mitochondria turnover in growing pollen tubes. Live-cell imaging and dynamic tracking analysis revealed that the spatiotemporal distributions of mitochondria and YFP-ATG8e mainly stayed separated with occasional colocalization (Figure 6). This may suggest that mitophagy in growing pollen tubes under normal conditions is likely to remain at a basic, low level.

2,4-dinitrophenol (DNP) has been used as a chemical agent to trigger mitophagy in mammalian and plant cells due to its function as an uncoupler, resulting in depolarized mitochondrial membrane [45,46]. After DNP treatment, it is noteworthy that YFP-ATG8e contacted and spatiotemporally associated with the depolarized mitochondria in growing pollen tubes (Figure 6). Therefore, mitophagy can be stimulated by uncoupler treatment in growing pollen tubes consistent with recent observations in *Arabidopsis* root cells [46]. In addition, kymographic analysis of YFP-ATG8e in association with the depolarized mitochondrion showed highly coordinated movement in pollen tubes (Figure 6). Importantly, disruption of the potential AIM-docking site of ATG8e abolished the contact and spatiotemporal coordination of ATG8e with the damaged mitochondria (Figure 6). The results illustrated that ATG8e could specifically interact with damaged mitochondria *via* AIM to mediate the mitophagy pathway in growing pollen tubes. This scenario is further supported by the TEM identification of mitophagosomes in *Arabidopsis* pollen tubes (Figure 7). Furthermore, the mitophagosomes identified within *Arabidopsis* pollen tubes in our study are morphologically comparable with the structure of mitophagosome in animal cells reported in previous studies [67,68].

## Materials and Methods

### Plant materials and growth

*Nicotiana tabacum* seeds were directly sowed in the soil for germination. Three weeks later, each juvenile plant was transferred into individual flowerpots and grown in the greenhouse at 28°C with a light cycle of 12-h light and 12-h darkness. *Arabidopsis thaliana* seeds were surface sterilized (70% ethanol and 0.2% Tween 20 for 10 min of vigorous vortex), rinsed twice with 100% ethanol and air dried on filter paper. The seeds were spread on Murashige and Skoog medium (Sigma-Aldrich, M5519) with 1% agar (Sangon Biotech, A100637), 1% sucrose (Fluka, 84,097) and vitamin mixture plate, and then stratified for 2 d at 4°C. The plates were transferred to a plant growth chamber and cultured vertically at 22°C under a light cycle of 16-h light and 8-h darkness for 7 d. Thereafter, seedlings were transferred to soil (Jiffy Products International, EN12580) and grown until harvested at the same growth conditions.

### In vitro and in vivo pollen germination

Tobacco pollen germination: fresh and mature tobacco pollens were selected and harvested before use as described previously [69]. For *in vitro* pollen tube germination, the pollen grains were suspended in tobacco pollen-specific germination medium containing 10% sucrose (Fluka, 84,097), 0.01% boric acid (Sigma-Aldrich, 202,878), 1 mM CaCl<sub>2</sub> (Ajax Chemicals, 960), 1 mM Ca(NO<sub>3</sub>)<sub>2</sub>·4 H<sub>2</sub>O (Sigma-Aldrich, C1396) and 1 mM MgSO<sub>4</sub>·7H<sub>2</sub>O (Sigma-Aldrich, M1880) at pH 6.5. The pollen was germinated at 27.5°C in an 85 rpm orbital rotary shaker for 2 h.

*Arabidopsis* pollen germination: i) *in vitro* pollen germination and collection of *Arabidopsis* flowers at the proper growth stage were conducted as previously described [69]. *Arabidopsis* pollen grains were released from anthers by vigorous vortex in *Arabidopsis* pollen germination medium containing 0.01% boric acid, 1 mM Ca(NO<sub>3</sub>)<sub>2</sub>, 1 mM MgSO<sub>4</sub>, 5 mM CaCl<sub>2</sub> and 18% (w:v) sucrose at pH 7.0. Thereafter, the petals and anthers were removed with forceps, and *Arabidopsis* pollen was centrifuged at 800 g for 1 min at room temperature (RT). The majority of the supernatant was removed with approximately 50 µl germination medium remaining in the tube. The pollen pellet was gently resuspended and 10–15 µl liquid droplets were placed onto glass slides. The slides were rapidly flipped upside down and let sit in a wet chamber box filled with wet Kimwipes and sealed tightly. The chamber box was incubated at 27°C for 4 h. ii) For the *in vivo* pollen germination, stage 12 *Arabidopsis* flowers were castrated and used as female. Pollen grains were collected from stage 15 flowers and applied to the stigma for pollination and pollen germination [70].

### Aniline blue staining of in vivo pollen tube growth assay

The staining experiment was performed as previously described [71]. In general, hand pollinated pistils were fixed with acetic acid:ethanol (1:3 v:v) solution for 2 h at RT. The

fixation solution was discarded, and the sample was hydrated with an ethanol series (70%, 50% and 30% ethanol) for 10 min each at RT. The samples were then washed with ddH<sub>2</sub>O and subsequently immersed in 4 M NaOH at 37°C for 3–4 h to allow softening and transparency. Finally, the sample was washed with ddH<sub>2</sub>O for 5 times, stained with 0.1% aniline blue (Sangon Biotech, A500083) and prepared in 0.1% K<sub>3</sub>PO<sub>4</sub> in the dark for 2 h before imaging.

### **Protein extraction and immunoblot detection**

Proteins were extracted from Arabidopsis mature pollen grains and 4-h germinated pollen tubes respectively. The extraction method followed a previous study for better detection of ATG8-lipid adduct [72]. Equal amounts of proteins were loaded to SDS-PAGE on 15% polyacrylamide gels with 6 M urea, and electrophoretically transferred onto polyvinylidene fluoride membranes. The ATG8-PE and free ATG8 were detected by immunoblot with anti-ATG8 antibodies (Abcam, ab77003).

### **Transient expression of chimeric fluorescent fusion proteins in growing tobacco pollen tubes**

In general, fresh tobacco anthers were harvested from 15–20 tobacco flowers. They were then transferred into a test tube containing 10 ml of pollen germination medium and vortexed vigorously to release pollen grains into the germination medium. The pollen grains were then prepared for transient expression of chimeric fluorescent fusion proteins in growing pollen tubes via particle bombardment. The procedures of biolistic bombardment and bio-imaging of live pollen tubes were performed as described [69,73].

### **Electron microscopy of the resin-embedded pollen tubes**

The general procedures for TEM sample preparation and ultra-thin sectioning of samples were performed as previously described [40]. For fixation of growing tobacco pollen tubes, high-pressure freezing and substitution were used as previously described [61,74]. Subsequent freeze substitution was carried out in dry acetone containing 0.1% uranyl acetate (Electron Microscopy Sciences, 22,400) at –85°C. Infiltration with HM20 (Electron Microscopy Sciences, 14,330–14,360), embedding, and UV polymerization were performed stepwise at –35°C. Images were collected by an FEI Talos transmission electron microscope.

### **Confocal laser scanning microscopy imaging and image analysis**

In general, the confocal fluorescence images were collected using a Leica TCS SP8 system with the following parameters: 63x water objective, 2x zoom, 750 gain, 0 background, 0.168 μm pixel size and photomultiplier tubes (PMTs) detector. The images from pollen tubes expressing fluorescent tagged proteins were collected with a laser level of ≤3% to ensure that the fluorescent signal was within the linear range of detection (typically 0.5 or 1% laser was used). Time-lapse images of growing pollen tubes were collected by continuing imaging with minimal time interval.

Colocalizations between two fluorescent proteins were calculated by Fiji program with PSC colocalization plug-in as described previously [75]. Briefly, fixed size region of interest (ROI) containing relevant signal information in both emission channels (one for each fluorophore) was performed on acquired confocal images. Results are presented either as Pearson correlation coefficients or as Spearman's rank correlation coefficients, both of which produce *r* values in the range (–1, 1), where 0 indicates no discernable correlation and +1 or –1 indicate strong positive or negative correlations, respectively.

Kymograph analysis was conducted by Imaris software (<https://imaris.oxinst.com/>). In general, original 2D time-lapse images of growing pollen tubes obtained by confocal microscopy were uploaded into Imaris. Then, the function to swap time and z axis of Imaris was selected to generate a time projection image. Subsequently, the image was flipped 90 degrees vertically to generate the kymograph of the entire growing pollen tube such that the x axis represents time and the y axis includes the stacks for all frames. Further The ROI was further selected using the crop 3D function of Imaris to demonstrate the dynamic motions of the intracellular proteins in growing pollen tubes.

Fiji is used for signal detection and counting of fluorescent proteins in pollen tubes. The images are processed by following particle analysis protocol from Fiji (<https://imagej.net/imaging/particle-analysis>). Besides, we further manually checked the accuracy of signal recognition between the protein puncta and software detections prior to particle counting analysis.

### **Chemicals and drug treatment**

Stock solutions of BTH (5 mM in methanol; Sigma-Aldrich, 32,820), DNP (10 mM in DMSO; Sigma-Aldrich, D198501) and wortmannin (1.65 mM in DMSO; Sigma-Aldrich, 681,676) were aliquoted and stored at –20°C. For each drug treatment, germinating pollen tubes were mixed with drugs in working solutions of germination medium at a 1:1 ratio to minimize sample variation.

### **Acknowledgments**

We apologize to the researchers in the field whose work could not be cited and discussed due to space limitations. We would like to thank Dr. Andrew Loria for help with editing. We also thank members of Wang laboratory for insightful discussion of the manuscript. This work is supported by grants from the National Natural Science Foundation of China (91954110 and 31770196) and the Natural Science Foundation of Guangdong Province (2021A1515012066) to H. W.

### **Disclosure statement**

The authors declare that they have no competing interests.

### **Funding**

This work was supported by the National Natural Science Foundation of China [31770196]; National Natural Science Foundation of China [91954110]; Natural Science Foundation of Guangdong Province [2021A1515012066].



## ORCID

Hao Wang  <http://orcid.org/0000-0002-1695-8825>

## References

- [1] Cai G, Parrotta L, Cresti M. Organelle trafficking, the cytoskeleton, and pollen tube growth. *J Integr Plant Biol.* 2015;57:63–78.
- [2] Dumais J. Mechanics and hydraulics of pollen tube growth. *New Phytol.* 2021;232(4):1549–1565.
- [3] Hepler PK, Vidali L, Cheung AY. Polarized cell growth in higher plants. *Annu Rev Cell Dev Biol.* 2001;17:159–187.
- [4] Selinski J, Scheibe R. Pollen tube growth: where does the energy come from? *Plant Signal Behav.* 2014;9:e977200.
- [5] Zhao LF, Rehmani MS, Wang H. Exocytosis and endocytosis: yin-yang crosstalk for sculpting a dynamic growing pollen tube tip. *Front Plant Sci.* 2020;11. DOI:10.3389/fpls.2020.572848.
- [6] Guo J, Yang Z. Exocytosis and endocytosis: coordinating and fine-tuning the polar tip growth domain in pollen tubes. *J Exp Bot.* 2020;71:2428–2438.
- [7] Cameron C, Geitmann A. Cell mechanics of pollen tube growth. *Curr Opin Genet Dev.* 2018;51:11–17.
- [8] Shimada T, Takagi J, Ichino T, et al. Plant vacuoles. *Annu Rev Plant Biol.* 2018;69:123–145.
- [9] Eisenach C, Francisco R, Martinoia E. Plant vacuoles. *Curr Biol.* 2015;25(4):136–137.
- [10] Hara-Nishimura I, Hatsugai N. The role of vacuole in plant cell death. *Cell Death Differ.* 2011;18:1298–1304.
- [11] Huang XR, Peng XB, Xie F, et al. The stereotyped positioning of the generative cell associated with vacuole dynamics is not required for male gametogenesis in rice pollen. *New Phytol.* 2018;218:463–469.
- [12] Ugalde JM, Rodriguez-Furlan C, De Rycke R, et al. Phosphatidylinositol 4-phosphate 5-kinases 1 and 2 are involved in the regulation of vacuole morphology during *Arabidopsis thaliana* pollen development. *Plant Sci.* 2016;250:10–19.
- [13] Hicks GR, Rojo E, Hong SH, et al. Geminating pollen has tubular vacuoles, displays highly dynamic vacuole biogenesis, and requires VACUOLESS1 for proper function. *Plant Physiol.* 2004;134:1227–1239.
- [14] Doherty J, Baehrecke EH. Life, death and autophagy. *Nat Cell Biol.* 2018;20:1110–1117.
- [15] Dundar G, Shao ZH, Higashitani N, et al. Autophagy mitigates high-temperature injury in pollen development of *Arabidopsis thaliana*. *Dev Biol.* 2019;456:190–200.
- [16] Farquharson KL. Autophagy contributes to plant lipid homeostasis. *Plant Cell.* 2019;31:1427–1428.
- [17] Signorelli S, Tarkowski LP, Van den Ende W, et al. Linking autophagy to abiotic and biotic stress responses. *Trends Plant Sci.* 2019;24:413–430.
- [18] Marshall RS, Vierstra RD. Autophagy: the master of bulk and selective recycling. *Annu Rev Plant Biol.* 2018;69:173–208.
- [19] Liu YM, Bassham DC. Autophagy: pathways for self-eating in plant cells. *Annu Rev Plant Biol.* 2012;63:215–237.
- [20] Hofius D, Lie L, Hafren A, et al. Autophagy as an emerging arena for plant-pathogen interactions. *Curr Opin Plant Biol.* 2017;38:117–123.
- [21] Yang C, Shen WJ, Yang LM, et al. HY5-HDA9 module transcriptionally regulates plant autophagy in response to light-to-dark conversion and nitrogen starvation. *Mol Plant.* 2020;13:515–531.
- [22] Hayward AP, Dinesh-Kumar SP. What can plant autophagy do for an innate immune response? *Annu Rev Phytopathol.* 2011;49:557–576.
- [23] Soto-Burgos J, Zhuang XH, Jiang LW, et al. Dynamics of autophagosome formation. *Plant Physiol.* 2018;176:219–229.
- [24] Zhao YG, Zhang H. Formation and maturation of autophagosomes in higher eukaryotes: a social network. *Curr Opin Cell Biol.* 2018;53:29–36.
- [25] Nguyen L, Montrasio F, Pattamatta A, et al. Antibody therapy targeting RAN proteins rescues C9 ALS/FTD phenotypes in C9orf72 mouse model. *Neuron.* 2020;105:645–662.
- [26] Zhuang XH, Wang H, Lam SK, et al. A BAR-domain protein SH3P2, which binds to phosphatidylinositol 3-phosphate and ATG8, regulates autophagosome formation in *Arabidopsis*. *Plant Cell.* 2013;25:4596–4615.
- [27] Beckers J, Tharkeshwar AK, Van Damme P. C9orf72 ALS-FTD: recent evidence for dysregulation of the autophagy-lysosome pathway at multiple levels. *Autophagy.* 2021;17:3306–3322.
- [28] Bu F, Yang MK, Guo X, et al. Multiple functions of ATG8 family proteins in plant autophagy. *Front Cell Dev Biol.* 2020;8. DOI:10.3389/fcell.2020.00466.
- [29] Norizuki T, Minamino N, Ueda T. Role of autophagy in male reproductive processes in land plants. *Front Plant Sci.* 2020;11. DOI:10.3389/fpls.2020.00756.
- [30] Li SH, Yan H, Mei WM, et al. Boosting autophagy in sexual reproduction: a plant perspective. *New Phytol.* 2020;226:679–689.
- [31] Hanamata S, Kurusu T, Kuchitsu K. Roles of autophagy in male reproductive development in plants. *Front Plant Sci.* 2014;5. DOI:10.3389/fpls.2014.00457.
- [32] Harrison-Lowe NJ, Olsen LJ. Autophagy protein 6 (ATG6) is required for pollen germination in *Arabidopsis thaliana*. *Autophagy.* 2008;4:339–348.
- [33] Kurusu T, Koyano T, Hanamata S, et al. OsATG7 is required for autophagy-dependent lipid metabolism in rice postmeiotic anther development. *Autophagy.* 2014;10:878–888.
- [34] Qin GJ, Ma ZQ, Zhang L, et al. Arabidopsis AtBECLIN1/AtAtg6/AtVps30 is essential for pollen germination and plant development. *Cell Res.* 2007;17:249–263.
- [35] Wipf P, Halter RJ. Chemistry and biology of wortmannin. *Org Biomol Chem.* 2005;3:2053–2061.
- [36] Zhao P, Zhou XM, Zhao LL, et al. Autophagy-mediated compartmental cytoplasmic deletion is essential for tobacco pollen germination and male fertility. *Autophagy.* 2020;16:2180–2192.
- [37] Ahn G, Kim H, Kim DH, et al. SH3 domain-containing protein 2 plays a crucial role at the step of membrane tubulation during cell plate formation. *Plant Cell.* 2017;29:1388–1405.
- [38] Wymann MP, Bulgarelli-Leva G, Zvelebil MJ, et al. Wortmannin inactivates phosphoinositide 3-kinase by covalent modification of Lys-802, a residue involved in the phosphate transfer reaction. *Mol Cell Biol.* 1996;16:1722–1733.
- [39] Miao YS, Yan PK, Kim H, et al. Localization of green fluorescent protein fusions with the seven Arabidopsis vacuolar sorting receptors to prevacuolar compartments in tobacco BY-2 cells. *Plant Physiol.* 2006;142:945–962.
- [40] Tse YC, Mo BX, Hillmer S, et al. Identification of multivesicular bodies as prevacuolar compartments in *Nicotiana tabacum* BY-2 cells. *Plant Cell.* 2004;16:672–693.
- [41] Wang H, Zhuang XH, Hillmer S, et al. Vacuolar sorting receptor (VSR) proteins reach the plasma membrane in germinating pollen tubes. *Mol Plant.* 2011;4:845–853.
- [42] Wang JQ, Cai Y, Miao YS, et al. Wortmannin induces homotypic fusion of plant prevacuolar compartments\*. *J Exp Bot.* 2009;60:3075–3083.
- [43] Lee Y, Bak G, Choi Y, et al. Roles of phosphatidylinositol 3-kinase in root hair growth. *Plant Physiol.* 2008;147:624–635.
- [44] Vermeer JEM, van Leeuwen W, Tobena-Santamaria R, et al. Visualization of PtdIns3P dynamics in living plant cells. *Plant J.* 2006;47:687–700.
- [45] Georgakopoulos ND, Wells G, Campanell M. The pharmacological regulation of cellular mitophagy. *Nat Chem Biol.* 2017;13:136–146.
- [46] Ma J, Liang Z, Zhao J, et al. Friendly mediates membrane depolarization-induced mitophagy in *Arabidopsis*. *Curr Biol.* 2021;31:1931–1944.
- [47] Maqbool A, Hughes RK, Dagdas YF, et al. Structural basis of host autophagy-related protein 8 (ATG8) binding by the Irish potato famine pathogen effector protein PexRD54. *J Biol Chem.* 2016;291:20270–20282.

- [48] Zhou X, Zhao P, Sun MX. Autophagy in sexual plant reproduction: new insights for thought. *J Exp Bot.* **2021**;72:7658–7667.
- [49] Safavian D, Goring D. Autophagy in the rejection of self-pollen in the mustard family. *Autophagy.* **2014**;10:2379–2380.
- [50] Tsukamoto S, Kuma A, Murakami M, et al. Autophagy is essential for preimplantation development of mouse embryos. *Science.* **2008**;321:117–120.
- [51] Kurusu T, Kuchitsu K. Autophagy, programmed cell death and reactive oxygen species in sexual reproduction in plants. *J Plant Res.* **2017**;130:491–499.
- [52] Kurusu T, Koyano T, Kitahata N, et al. Autophagy-mediated regulation of phytohormone metabolism during rice anther development. *Plant Signal Behav.* **2017**;12:e1365211.
- [53] Zhang Y, Li S, Zhou LZ, et al. Overexpression of *Arabidopsis thaliana* PTEN caused accumulation of autophagic bodies in pollen tubes by disrupting phosphatidylinositol 3-phosphate dynamics. *Plant J.* **2011**;68:1081–1092.
- [54] Zhou XM, Zhao P, Wang W, et al. A comprehensive, genome-wide analysis of autophagy-related genes identified in tobacco suggests a central role of autophagy in plant response to various environmental cues. *DNA Res.* **2015**;22:245–257.
- [55] Zhuang XH, Cui Y, Gao CJ, et al. Endocytic and autophagic pathways crosstalk in plants. *Curr Opin Plant Biol.* **2015**;28:39–47.
- [56] Gao CJ, Zhuang XH, Cui Y, et al. Dual roles of an Arabidopsis ESCRT component FREE1 in regulating vacuolar protein transport and autophagic degradation. *Proc Natl Acad Sci U S A.* **2015**;112:1886–1891.
- [57] Abdulrahman BA, Abdelaziz DH, Schatzl HM. Autophagy regulates exosomal release of prions in neuronal cells. *J Biol Chem.* **2018**;293:8956–8968.
- [58] Liu F, Hu WM, Li FQ, et al. AUTOPHAGY-RELATED14 and its associated phosphatidylinositol 3-Kinase complex promote autophagy in Arabidopsis. *Plant Cell.* **2020**;32:3939–3960.
- [59] Zhong GT, Zhu QL, Li YX, et al. Once for all: a novel robust system for co-expression of multiple chimeric fluorescent fusion proteins in plants. *Front Plant Sci.* **2017**;8. DOI:10.3389/fpls.2017.01071.
- [60] Chung T. How phosphoinositides shape autophagy in plant cells. *Plant Sci.* **2019**;281:146–158.
- [61] Wang H, Zhuang XH, Cai Y, et al. Apical F-actin-regulated exocytic targeting of NtPPME1 is essential for construction and rigidity of the pollen tube cell wall. *Plant J.* **2013**;76:367–379.
- [62] Gao C, Luo M, Zhao Q, et al. A unique plant ESCRT component, FREE1, regulates multivesicular body protein sorting and plant growth. *Curr Biol.* **2014**;24:2556–2563.
- [63] Kim JH, Lee HN, Huang X, et al. FYVE2, a phosphatidylinositol 3-phosphate effector, interacts with the COPII machinery to control autophagosome formation in Arabidopsis. *Plant Cell.* **2021**;34:351–373.
- [64] Broda M, Millar AH, Van Aken O. Mitophagy: a mechanism for plant growth and survival. *Trends Plant Sci.* **2018**;23:434–450.
- [65] Moehlman AT, Youle RJ. Mitochondrial quality control and restraining innate immunity. *Annu Rev Cell Dev Biol.* **2020**;36:265–289.
- [66] Warmke HE, Lee SL. Pollen abortion in T cytoplasmic male-sterile corn (*Zea mays*): a suggested mechanism. *Science.* **1978**;200:561–563.
- [67] Luciani A, Schumann A, Berquez M, et al. Impaired mitophagy links mitochondrial disease to epithelial stress in methylmalonyl-CoA mutase deficiency. *Nat Commun.* **2020**;11
- [68] Okamoto K, Kondo-Okamoto N, Ohsumi Y. Mitochondria-anchored receptor Atg32 mediates degradation of mitochondria via selective autophagy. *Dev Cell.* **2009**;17:87–97.
- [69] Zhong G, Liu R, Zhuang M, et al. Transient expression of chimeric fluorescent reporter proteins in pollen tubes to study protein polar secretion and dynamics. *Methods Mol Biol.* **2017**;1662:115–124.
- [70] Smyth DR, Bowman JL, Meyerowitz EM. Early flower development in Arabidopsis. *Plant Cell.* **1990**;2(8):755–767.
- [71] Mori T, Kuroiwa H, Higashiyama T, et al. GENERATIVE CELL SPECIFIC 1 is essential for angiosperm fertilization. *Nat Cell Biol.* **2006**;8:64–71.
- [72] Chung T, Phillips AR, Vierstra RD. ATG8 lipidation and ATG8-mediated autophagy in Arabidopsis require ATG12 expressed from the differentially controlled ATG12A and ATG12B loci. *Plant J.* **2010**;62:483–493.
- [73] Wang H, Jiang LW. Transient expression and analysis of fluorescent reporter proteins in plant pollen tubes. *Nat Protoc.* **2011**;6:419–426.
- [74] Wang H, Zhuang XH, Wang XF, et al. A distinct pathway for polar exocytosis in plant cell wall formation. *Plant Physiol.* **2016**;172:1003–1018.
- [75] French AP, Mills S, Swarup R, et al. Colocalization of fluorescent markers in confocal microscope images of plant cells. *Nat Protoc.* **2008**;3:619–628.